12 The interstellar medium

Before a spacecraft encounters its target star, it must pass through our solar system and cross the vast extent of interstellar space. At a few hundred astronomical units from the Sun, the spacecraft will cross the edge of the heliosphere, where the interstellar medium (ISM) begins to dominate the solar wind emitted by the Sun. The ISM is not empty, and the spacecraft will encounter gas and dust particles at high speeds. We examine the impact of such particles on the spacecraft, quantify the damage they would make, and look at mitigating actions. We will also see how the concept of the Bussard ramjet could, in principle, exploit the ISM particles as a source of fuel and propellant. When arriving at its target star, the spacecraft can study its heliosphere, and look for analogues to the minor bodies in our own solar system.

12.1 The solar system

What will an interstellar spacecraft encounter as it leaves our solar system?

To acquire its large velocity, a spacecraft may first dive very close to the Sun, either as a rocket to take advantage of the Oberth effect (section 4.2.3), or as a solar sail to benefit from the higher photon intensity (section 10.7). The spacecraft could even pass close to a planet to perform a gravity assist (section 4.3), primarily to change its direction of travel because this manoeuvre would not add significantly to the otherwise very large velocity we are aiming for.

In many cases, though, our interstellar spacecraft will avoid the Sun and the planets. The spacecraft may pass through the asteroid belt. This has such a low number density that the probability of a collision with an unmapped object is negligible.

Beyond the orbit of Neptune there is a large population of minor planets and comets organized into various classes according to their orbits and properties. One of these classes is the Kuiper belt, objects lying mostly at distances of 30–50 au, the best and longest-known member of which is Pluto. Some of these objects, including Pluto, are in resonant orbits with Neptune. Another class of minor planets is the scattered disk objects, which have eccentric and inclined non-resonant orbits. The largest of these is Eris, which is currently the most massive trans-Neptunian object known ($0.0027\,M_\oplus$), with aphelion and perihelion distances of 98 au, and 38 au, respectively. In total there are of the order of 10^5 trans-Neptunian objects larger than 100 km, and probably of the order of 10^{11} larger than 1 km. Yet their total mass is perhaps only $0.1\,M_\oplus$. Our interstellar spacecraft could possibly be steered to examine one of these, perhaps as a test of how to do science observations during a high-speed encounter.

Beyond the scattered disk there lies a large population of comets with aphelia extending up to 0.25 pc or more, the Oort cloud. No Oort cloud objects have been directly observed

Downloaded from https://www.cambridge.org/core. UNIVERSIDAD AUTONOMA METROPOLITANA, on 13 Nov 2026 at 09:32:29, subject to the Cambridge Core terms of use, available at https://www.cambridge.org/core/terms. https://doi.org/10.1017/9781009700429.013

in situ, but gravitational interactions with passing stars (or with the stellar population as a whole in the form of the Galactic tide), can push them into the inner parts of the solar system, where their orbits can be further perturbed by Jupiter. This is believed to be the source of long-period comets (longer than 200 yr). Estimates of the size of the Oort cloud are highly uncertain, but there are perhaps 10^{12} objects of radius 1 km, which at a typical comet density of 500 kg m^{-3} implies a mass of 2×10^{24} kg or 0.35 $M_\oplus$, but this could easily be out by an order of magnitude. If their masses are distributed like other solar system bodies, then most of the mass will be in the few largest objects. In any case, given the vast volume they are spread over, the probability of a transiting spacecraft colliding with any of them is negligible (see exercises). Correspondingly, the closest expected flyby distance to any one of them is a few astronomical units (if they all had the same size). Given the extreme faintness of Oort cloud objects both in reflected sunlight and in the thermal infrared, it is unlikely a single spacecraft would have the opportunity to observe one as it flies through.

12.2 The solar wind and its interaction with the interstellar medium

The outermost part of the Sun's atmosphere is the corona, visible to the naked eye during a solar eclipse as a set of jagged structures extending beyond the otherwise near-spherical surface of the Sun. The corona has a low density but is heated to $1–2 \times 10^6$ K by magnetic fields and is therefore completely ionized. Some of this plasma has enough energy to overcome the Sun's gravity and streams away as the solar wind.

The solar wind comprises mostly protons (hydrogen ions) and electrons with some helium nuclei (2–4% by number) and heavier ions. Overall the solar wind is neutral. As a charged fluid that supports pressure, its individual particles move not only under the force of gravity. A simple hydrodynamical model of the solar wind shows that it initially accelerates away from the Sun. Considering just the protons (as these dominate the mass), this model shows that the solar wind becomes supersonic after a few solar radii. The wind has a range of temperatures (and thus energies), but for wind at 10^6 K, it continues to accelerate out to about 40 $R_\odot$ (0.19 au), reaching a velocity of 400–500 km s^{-1}, after which it maintains a more or less constant velocity out to large distances.

Observations show that the particles in the solar wind can be divided into two distinct populations of different energies and densities. At 1 au from the Sun, the so-called fast solar wind has a velocity between 400 km s^{-1} and 800 km s^{-1} and an ion flux density of 2×10^{12} m^{-2} s^{-1}, corresponding to a ion number density of $2.5–5 \times 10^6$ m^{-3}. The proton temperature is about 2×10^5 K; the electron temperature is half this. The fast solar wind comes primarily from coronal holes, which are cooler regions that emit less ultraviolet and X-ray radiation. The so-called slow solar wind originates mostly from the equatorial regions of the Sun. This component has velocities of 250–400 km s^{-1}, about twice as dense as the fast solar wind, and it has a lower proton temperature, about 3×10^4 K. The total solar wind (fast and slow) ion density varies with time, but at 1 au it is around 10^7 m^{-3} on average. This corresponds to a mass loss rate from the Sun of a few 10^{-14} $M_\odot$ yr^{-1}.

The dynamic pressure, or ram pressure, exerted by the solar wind is $(1/2)\rho v^2$, where ρ is its mass density and v its velocity. Adopting a particle number density of 1×10^7 m^{-3} and

Downloaded from https://www.cambridge.org/core. UNIVERSIDAD AUTONOMA METROPOLITANA, on 13 Nov 2026 at 09:32:29, subject to the Cambridge Core terms of use, available at https://www.cambridge.org/core/terms. https://doi.org/10.1017/9781009700429.013

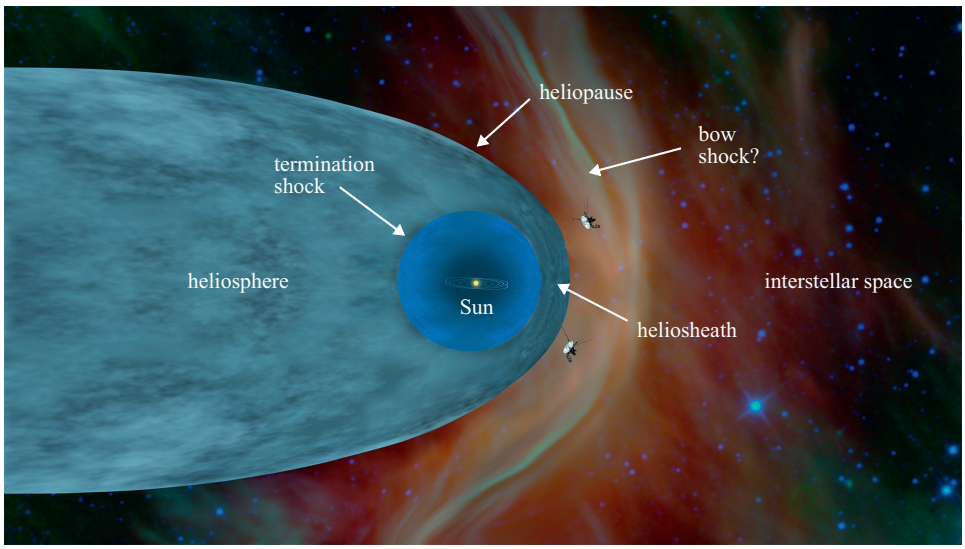


Fig. 12.1 The heliosphere and the edge(s) of the solar system. Credit: Courtesy NASA/JPL-Caltech, annotated by the author.

assuming the solar wind is all protons moving at 400 km s^{-1}, the ram pressure is 1×10^{-9} Pa. This is several thousand times less than the solar photon pressure at 1 au (section 10.1).

The Sun itself also has a magnetic field. Because the solar wind is highly conductive, the solar magnetic field is coupled to the wind and dragged along with it. This is wound into spirals by the rotation of the Sun. The magnetic field strength is a few nanoteslas at 1 au.

The *heliosphere* is that region of space that is occupied by the solar wind and can be considered as a very low-density extension of the solar atmosphere. As the solar wind pressure decreases with distance from the Sun, there comes a point at which this pressure drops to the pressure of the gas in the ISM. The surface at which this occurs is the *heliopause*, the boundary of the heliosphere with interstellar space. If the Sun where stationary with respect to the ISM, the heliopause would be roughly spherical (although not exactly because the solar wind is neither isotropic nor constant in time). But due to the motion of the Sun with respect to the ISM, the heliosphere is expected to be compressed in the 'upwind' direction (the solar apex) and have an extended tail in the 'downwind' direction (solar antapex), as shown in figure 12.1, although some observational evidence suggests it is in fact more symmetric.

Voyager 1 became the first spacecraft to cross the heliopause in August 2012 when it detected a significant decrease in the ambient particle density. It was 121 au from the Sun at the time, and was travelling in the direction RA = 263°, Dec. = 12°, which is close to the solar apex (RA = 275°, Dec. = 30°). Voyager 2 crossed the heliopause in November 2018 at the same distance, travelling in nearly a perpendicular direction (RA = 316°, Dec. = −68°). So 120 au is a reasonable estimate for the distance to the heliopause at the solar apex. It possibly extends to tens of thousands of astronomical units in the antapex direction.

The heliopause is often taken as the definition of the edge of the solar system, although the Voyager spacecraft passed another edge some years earlier. This was the *termination shock*, defined as the boundary where the solar wind speed drops from supersonic to subsonic due to interactions with the ISM. Voyager 1 crossed the termination shock 94 au from the Sun,

Downloaded from https://www.cambridge.org/core. UNIVERSIDAD AUTONOMA METROPOLITANA, on 13 Nov 2026 at 09:32:29, subject to the Cambridge Core terms of use, available at https://www.cambridge.org/core/terms. https://doi.org/10.1017/9781009700429.013

Voyager 2 at 84 au. The location of the termination shock is probably variable in time too, as Voyager 2 seemed to cross it several times over the course of several hours.

Between the termination shock and the heliopause is the *heliosheath* (figure 12.1). This is the region of the heliosphere that is influenced by the ISM. The plasma here has a higher temperature and density than the solar wind internal to the termination shock. Observations from Voyager indicate that this region is not homogenous.

Finally, beyond the heliopause, there may exist a bow shock. This is where the velocity of the ISM relative to the solar wind drops from supersonic to subsonic (i.e. drops below the ISM speed of sound) due to the interaction with the heliosphere, creating turbulence. Bow shocks have been observed around other stars. It has been hypothesized that the solar bow shock is about 230 au from the Sun in the apex direction. The International Boundary Explorer (IBEX), which observes the heliosphere from an orbit near to the Earth using energetic neutral atoms, measured the velocity of the local ISM relative to the Sun to be $23.2\,\mathrm{km\,s^{-1}}$. This implies the pressure from the ISM is too low to produce a bow shock, and that there is instead an unshocked region of higher density. A suitably equipped interstellar spacecraft could shed some light on this issue (see chapter 16).

12.3 Composition of the interstellar medium

The space between the stars is not empty. In the ISM there are photons, neutral atoms, ions, electrons, molecules, dust and larger particles, as well as electric and magnetic fields generated by the charged particles. Evidence for matter in the ISM comes from both broad band absorption and reddening of starlight due to dust, and also from atomic and ionic spectroscopic absorption lines at characteristic wavelengths. Particle densities vary across space, and are not precisely determined, so some of the numbers given below may not be entirely self-consistent.

12.3.1 Atoms, ions, and electrons

The early universe consisted mostly of hydrogen and helium (from big bang nucleosynthesis), but after the first stars formed, nuclear fusion created heavier elements from these building blocks.[1] These elements are returned to the ISM through various processes, including stellar winds and more energetic events such as core-collapse (type II) supernovae or the merger of a white dwarf with another star in a binary system (type Ia supernovae).

The density and composition of the ISM varies by orders of magnitudes depending on location in the Galaxy, in particular the proximity to star forming regions. Interstellar material collapsing under gravity to form new stars can reach such high densities that they form clouds that are optically thick, with the protostars themselves barely visible (in the optical, at least). The nearest star-forming regions lie a few hundred light years from the Sun, so are unlikely to be the first targets of interstellar travel.

[1] This includes both fusion in the cores of stars to produce elements up to the iron/nickel peak (see figure 8.1), as well as proton and neutron capture processes in giant stars and core-collapse supernovae that create heavier elements.

Downloaded from https://www.cambridge.org/core. UNIVERSIDAD AUTONOMA METROPOLITANA, on 13 Nov 2026 at 09:32:29, subject to the Cambridge Core terms of use, available at https://www.cambridge.org/core/terms. https://doi.org/10.1017/9781009700429.013

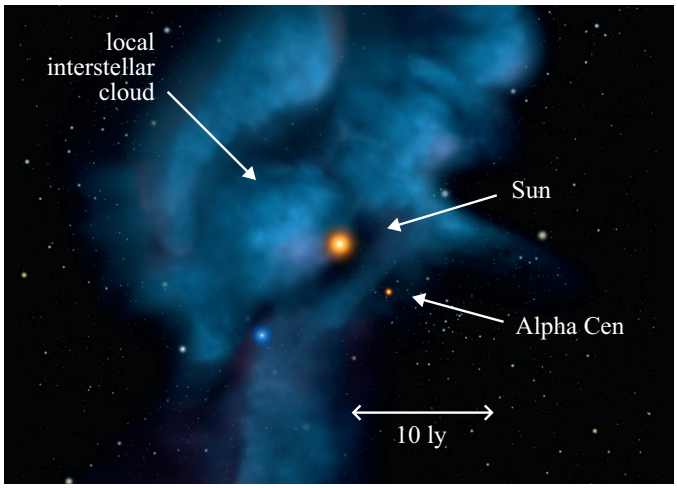


Fig. 12.2 The local ISM. Credit: NASA/Goddard/Adler/U. Chicago/Wesleyan, cropped and re-annotated by the author.

In regions far from stars and star-forming regions, the typical number density of the ISM is of the order of 10^6 gas atoms per cubic metre, or one per cubic centimetre. Most of these atoms are hydrogen. By number, hydrogen makes up about 90% of the atoms, most of the rest being helium, with about 0.1% heavier elements, mostly carbon, nitrogen, and oxygen. By mass, these correspond to 70% hydrogen, 28% helium, and 2% for the rest (which astronomers refer to collectively and confusingly as 'metals'). With this composition, a number density of $10^6\,\mathrm{m}^{-3}$ corresponds to a mass density of about $2 \times 10^{-21}\,\mathrm{kg\,m}^{-3}$. The density can be four orders of magnitude larger in denser clouds.

Interestingly, the Sun is in or at the edge of a lower than average density region known as the *local interstellar cloud*, a region roughly 10 pc (30 ly) across with a gas atom number density of about $0.3 \times 10^6\,\mathrm{m}^{-3}$ (figure 12.2). This cloud is embedded within the even lower density *local bubble*, an irregularly shaped region extending 50–200 pc from the Sun with a gas atom number density of just $0.05 \times 10^6\,\mathrm{m}^{-3}$. The local bubble was probably carved out by one or many supernova over the past several million years.

Not all of the atoms in the ISM are neutral, as some atoms are ionized by short wavelength radiation from stars, in particular hot OB stars. The ionization fraction in the ISM therefore depends on the proximity to such stars. At the edge of the solar system, about 25% of the hydrogen atoms are ionized. About 40% of helium atoms are ionized, with a very small fraction (less than 1%) doubly ionized. Given that helium has a higher first ionization energy than hydrogen – 24.6 eV vs 13.6 eV – it might seem surprising that helium shows a higher ionization fraction. The reason appears to be that whereas the hydrogen is ionized mostly by continuum starlight emission (at wavelengths below 91 nm), the helium is ionized primarily by very short wavelength emission lines (below 50 nm) coming from the hot gas phase of the ISM (see below).

As there are ions in the ISM, there must also be electrons. Overall the ISM is neutral, so the average electron number density must be similar to the ion density (accounting for multiple ionizations). Absorption line data combined with photoionization models of the very nearby ISM indicate that the electron number density is about $0.06 \times 10^6\,\mathrm{m}^{-3}$. Like

Downloaded from https://www.cambridge.org/core. UNIVERSIDAD AUTONOMA METROPOLITANA, on 13 Nov 2026 at 09:32:29, subject to the Cambridge Core terms of use, available at https://www.cambridge.org/core/terms. https://doi.org/10.1017/9781009700429.013

the ion density, this too varies significantly. The low density of the ions and electrons means collisions between them are rare, so they form a free-moving plasma. The electrons can be excited by electromagnetic waves of frequencies at or below the electron plasma frequency $\nu_p = \sqrt{n_e e^2/4\pi^2\epsilon_0 m_e}$, where m_e is the electron mass and n_e is the electron number density. This can be written more conveniently as $\nu_p = 9\sqrt{n_e}$ Hz. With $n_e = 10^6\,\mathrm{m}^{-3}$ we get a plasma frequency of $\nu_p = 9\,\mathrm{kHz}$. Waves with a frequency below this will be strongly dispersed by the ISM, making it effectively opaque. As an aside, the Earth's ionsphere has an electron density of around $n_e = 10^{12}\,\mathrm{m}^{-3}$, so is opaque to frequencies below 9 MHz. Thus radio waves at lower frequencies coming from astronomical objects (or interstellar spacecraft) are not observable from the ground. As the ions in the plasma are much more massive than the electrons, their plasma frequency is much lower.

12.3.2 Molecules, dust, and rocks

The hydrogen in the ISM will bind as molecular hydrogen (H_2) if the temperature is low enough and the density high enough. These conditions occur in molecular clouds, which is where new stars form out of the ISM. Under the right conditions, in particular in the absence of strong ultraviolet radiation, molecules of other elements can also form, including the hydroxyl radical (OH), carbon monoxide, water, ammonia (NH_3), and formaldehyde (H_2CO). Over 100 different molecules have been discovered in the ISM, including quite complex organic molecules comprising many atoms.

The ISM is filled also with dust particles. This is both dust that was formed in the ISM through the conglomeration of atoms, and dust that was formed around stars and then blown out by stellar radiation pressure. Interstellar dust particles have a broad range of masses with a mean around 10^{-16} kg. As the Sun is moving through the ISM, interstellar dust can be detected within the solar system, and has been measured by various interplanetary spacecraft, in particular Cassini. This found that dust is made of a range of elements, including carbon, magnesium, calcium, silicon, oxygen, and iron often in the form of silicates. Adopting a characteristic density of $2500\,\mathrm{kg\,m}^{-3}$, a spherical dust particle of mass 10^{-16} kg has a diameter of $0.4\,\mu\mathrm{m}$.

Dust particle masses extend down to at least 10^{-18} kg, probably further, and extend up to 10^{-12} kg, corresponding to a diameter of $10\,\mu\mathrm{m}$, although there are proportionally fewer large particles. The mass distribution has a small tail towards even larger masses. There is no clear definition of where dust stops and larger solid particles start, but 1 mm is sometimes taken as a cut-off. The number density of dust particles in the ISM ranges from $10^{-8}\,\mathrm{m}^{-3}$ to $10^{-5}\,\mathrm{m}^{-3}$. Taking an average number density of $10^{-7}\,\mathrm{m}^{-3}$ and an average mass per particle of 10^{-16} kg, the mass density of dust in the ISM is of order $10^{-23}\,\mathrm{kg\,m}^{-3}$, a hundred times less than the atomic density of $10^{-21}\,\mathrm{kg\,m}^{-3}$ given earlier. This is at best an order of magnitude estimate, and both atom and dust number densities vary considerably across space. But broadly speaking, dust makes up about 1% of the microscopic mass in the ISM (a fraction widely adopted in astronomy). The number and mass densities of atoms and dust are summarized in Table 12.1.

Moving up in size, interstellar rocks of centimetre or metre sizes presumably exist, but have never been detected. Once we get to objects ranging from tens of metres to kilometres in size, we are in the realm of interstellar meteoroids, asteroids, or comets, which can be individually imaged if they come close enough to the Sun. As of mid 2025, only three

Downloaded from https://www.cambridge.org/core. UNIVERSIDAD AUTONOMA METROPOLITANA, on 13 Nov 2026 at 09:32:29, subject to the Cambridge Core terms of use, available at https://www.cambridge.org/core/terms. https://doi.org/10.1017/9781009700429.013

Table 12.1 Number and mass densities of gas atoms (all ionization states) and dust particles in different parts of the ISM. Gas number densities are measured. Gas mass densities have been derived from these values, adopting an average atom mass of 2.1×10^{-27} kg (1.26 protons). Typical ISM' refers to regions far from stars and star-forming regions. The measured number densities vary considerably, by three orders of magnitude for dust, so the gas density listed here is an approximate average. The gas density in the local bubble and local interstellar cloud are better determined. The dust number and mass densities have been derived from the gas densities assuming a gas-to-dust mass ratio of 100 and an average dust particle mass of 10^{-16} kg

Region	Particle	Number density $[m^{-3}]$	Mass density $[\times 10^{-24}\,kg\,m^{-3}]$
Typical ISM	Gas	1×10^{6}	2000
	Dust	20×10^{-8}	20
Local bubble	Gas	0.05×10^{6}	100
	Dust	1×10^{-8}	1
Local interstellar cloud	Gas	0.3×10^{6}	600
	Dust	6×10^{-8}	6

such interstellar objects (ISOs) have been found (in 2017, 2019, and 2025): the very flattened object 1I/'Omuamua[2], with a disk diameter of around 100 m, and the interstellar comet 2I/Borisov, with a nucleus size of around 500 m. The larger comet 3I/ATLAS was only just discovered at the time of writing. All three were observed when relatively near to the Sun. They could be identified as interstellar in origin from their hyperbolic orbits, and from having ruled out the possibility that a close encounter with a planet modified the orbit of what was previously a bound solar system object. Based on just three detections obtained from different surveys, we can only estimate the space density of such objects to within an order of magnitude. But taking into account the selection effects of the survey that found 'Omuamua, one study concluded that there are of the order of $0.2\,au^{-3}$ objects of 'Omuamua size or larger near the Sun at any time.

The neutral atoms, ions, and dust particles in the ISM are moving with respect to one another, and so have a non-zero temperature (which, from the kinetic theory of gases, is proportional to the root mean square velocity dispersion). They absorb energy from starlight and re-emit it at various wavelengths (dust thermally; atoms through line emission). The ISM is often described as comprising several phases at different temperatures. These are relevant to astrophysical processes in the ISM. The warm neutral ISM, for example, has a temperature of around 8000 K, which corresponds to a velocity dispersion of $14\,km\,s^{-1}$ for hydrogen, from $(1/2)m\overline{v^2} = (3/2)kT$. This velocity dispersion is much smaller than the velocity of a fast interstellar spacecraft relative to the ISM. It is therefore this relative motion, rather than the thermal motion of the gas, that will generate a high energy flux of particles on the spacecraft. We consider the effects of this in section 12.4 below.

[2] Despite some excitement and inevitable speculation at the time, there was no good evidence to suggest this is an alien spacecraft as opposed to a natural object.

Downloaded from https://www.cambridge.org/core. UNIVERSIDAD AUTONOMA METROPOLITANA, on 13 Nov 2026 at 09:32:29, subject to the Cambridge Core terms of use, available at https://www.cambridge.org/core/terms. https://doi.org/10.1017/9781009700429.013

12.3.3 Cosmic rays and magnetic fields

The final material component of the ISM is Galactic cosmic rays. These are mostly ions with very high energies, ranging from 1 GeV to 10^{11} GeV or more (kinetic plus rest energy). They arise from a range of high-energy astronomical phenomena, in particular supernovae and black hole accretion disks. The distribution of cosmic rays is roughly isotropic in the Galaxy's rest frame, probably due to the action of interstellar magnetic fields. Cosmic rays are mostly protons and helium nuclei, but around 1% are heavier nuclei (ions). Their flux is largest at 1 GeV, where it is of the order of $2 \times 10^4\,\mathrm{s^{-1}\,m^{-2}\,str^{-1}\,GeV^{-1}}$. The number per unit energy decreases with increasing energy E as approximately $E^{-2.7}$. A 1 GeV proton has a velocity of $0.26\,c$, so unlike the rest of the ISM constituents, cosmic rays will hit even a fast spacecraft from all directions.

As interstellar space is full of ions and electrons, we would also expect it to be permeated with magnetic fields. The strength of magnetic fields can be measured in the radio by Faraday rotation. There is a large variation, but a reasonable average field strength is 5×10^{-10} T. In the local interstellar cloud, calculations suggest the field strength is $2\text{–}5 \times 10^{-10}$ T. These compare to the Earth's magnetic field at the surface of around 5×10^{-5} T.

12.4 Impacts on a spacecraft

12.4.1 Collision rates

A spacecraft moving at velocity v relative to the ISM experiences a flux of neutral atoms, ions, and dust particles with a range of kinetic energies. With cross-sectional area A, the spacecraft passes through a volume Avt in time t. When the volume number density of particles is n, the spacecraft will encounter $Anvt$ particles in this time.[3] Thus the flux of particles – the number per unit cross-sectional area per second – is nv. With $n = 0.3 \times 10^6\,\mathrm{m^{-3}}$ – typical of gas atoms in the local interstellar cloud from table 12.1 – and $v = 0.1\,c$, the flux is $9 \times 10^{12}\,\mathrm{m^{-2}\,s^{-1}}$, corresponding to a mass flux of the order of $2 \times 10^{-14}\,\mathrm{kg\,m^{-2}\,s^{-1}}$. Over a distance x, the total number of particle impacts per unit area is nx. For the 4.25 ly journey to Proxima Cen, this gives a total number of impacted gas atoms of $1 \times 10^{22}\,\mathrm{m^{-2}}$, which corresponds to a gas mass of $2 \times 10^{-5}\,\mathrm{kg\,m^{-2}}$. The number of dust particles impacting the spacecraft over this journey is $2 \times 10^9\,\mathrm{m^{-2}}$ (adopting $n = 6 \times 10^{-8}\,\mathrm{m^{-3}}$) corresponding to a mass of $2 \times 10^{-7}\,\mathrm{kg\,m^{-2}}$, 100 times less than gas.

The above estimate applies when the number of particles encountered is much larger than one. This is not the case for very large objects, such as asteroids in the asteroid belt, Oort cloud comets, or ISOs. The average number of objects encountered over a path of length x is Anx. The probability of there being k encounters is described by the Poisson distribution:

$$P(k) = \frac{e^{-Anx}(Anx)^k}{k!}\,. \tag{12.1}$$

[3] This assumes that the velocity dispersion of the particles is much less than v, so we can consider the spacecraft moving at velocity v relative to every particle.

Downloaded from https://www.cambridge.org/core. UNIVERSIDAD AUTONOMA METROPOLITANA, on 13 Nov 2026 at 09:32:29, subject to the Cambridge Core terms of use, available at https://www.cambridge.org/core/terms. https://doi.org/10.1017/9781009700429.013

The average distance travelled between encounters, the mean free path, is $1/An$. The probability of $k = 0$ encounters is $\exp(-Anx)$, so the probability of one or more encounters is $1 - \exp(-Anx)$. For $Anx \ll 1$ we can use a Taylor expansion to see that this probability is[4]

$$P(k > 0) \simeq Anx \quad (Anx \ll 1) \,. \tag{12.2}$$

Consider ISOs with a space density of $0.2\,\mathrm{au}^{-3}$. Assume these are larger than our spacecraft and so dominate the collisional cross-sectional area, which I take as $\pi \times 500^2\,\mathrm{m}^2$; this is a rough guess so our result is only good to within a couple of orders of magnitude. Over a journey to Proxima Cen, the probability of one or more collisions with an ISO is then of order 10^{-12}, which is not worth worrying about. The probability of hitting an Oort cloud comet when leaving the solar system is likely to be even lower (see exercises). The probability of hitting an asteroid in the solar system's asteroid belt if flying through it is higher, perhaps of the order of 10^{-9}, but is still tiny.

Although we can neglect the possibility of a collision with such large objects, we do need to consider the damage that microscopic dust particles and atoms could do to the spacecraft. As the spacecraft will be moving much faster than the velocity dispersion within the ISM, essentially all of the high-energy impacts will take place on the surface in the direction of travel. The exception to this is cosmic rays.

12.4.2 Damage by atoms and ions

Incident neutral atoms or ions from the ISM will interact with the atoms in the solid material of the spacecraft. This occurs at the atomic level in the form of electromagnetic interactions between the incoming nucleus (plus its electrons if it is not fully ionized) and the the nuclei and electrons of the material. At low energies, the incoming atom interacts with both the nucleus and its bound electrons, and – if the material is a conductor – the free electrons. At kinetic energies above about 1 MeV, the cross-section for interactions of the incoming atom with a nucleus is much smaller than its cross-section for interactions with the material's electrons, so we need only consider the latter. As a hydrogen ion moving at $0.1\,c$ relative to the spacecraft has a kinetic energy of 4.7 MeV, this is the regime that dominates for high-speed interstellar travel. Furthermore, at energies above 1 MeV, an incoming ISM atom will be ionized completely by its initial interactions with the material (see figure 12.3). The electrons so stripped off will also impact the material, but as the electrons have masses and thus energies three to five orders of magnitude less than ions of the same initial speed, their impact effects can mostly be ignored, with the possible exception of bremsstrahlung, covered later. Thus at the typical velocities of the order of $0.1\,c$ for interstellar spacecraft, we consider mostly the interactions between incoming ions and the electrons in the spacecraft material.

The incident ion transfers energy to the atoms in the impacted material. This excites or ionizes the atoms. In the latter case, the secondary electrons transfer energy to neighbouring atoms. When these electrons recombine, they also release energy in the form of photons. In this way the energy of the impacting ion is dissipated through the material, primarily along a long thin track in the direction of travel. Most of this energy heats the material, and this may be enough to cause local melting. When the melted material later cools and solidifies, it likely does so into a different configuration, resulting in permanent damage to the structure.

[4] The probability of exactly one encounter is more or less identical when $Anx \ll 1$.

Downloaded from https://www.cambridge.org/core. UNIVERSIDAD AUTONOMA METROPOLITANA, on 13 Nov 2026 at 09:32:29, subject to the Cambridge Core terms of use, available at https://www.cambridge.org/core/terms. https://doi.org/10.1017/9781009700429.013

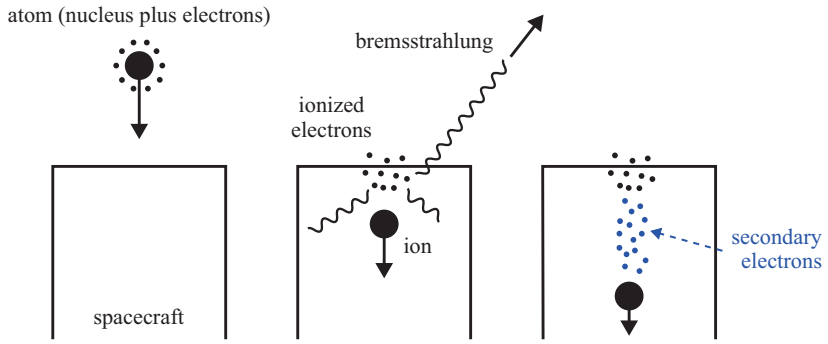


Fig. 12.3

A schematic of a collision of a high-velocity atom with a solid. The atom becomes fully ionized before it penetrates deeply into the solid; some of its electrons may be ejected from the surface. These decelerating electrons radiate their kinetic energy as bremsstrahlung. The ion penetrates more deeply into the solid, interacting primarily with the atomic electrons in the material (and free electrons if it is a conductor) and loses kinetic energy. This energy excites the electrons, heating the material, which may locally melt and lead to permanent track damage. Some atomic electrons may even become unbound (secondary electrons).

The energy may even be enough to vaporize the surface, leading to the loss of material. A penetrating particle can also displace an atom or ion, setting off a cascade of collisions. If these reach the surface, atoms can be ejected from the surface, a phenomenon known as sputtering.

When an ion penetrates a solid material, the rate at which the ion loses kinetic energy can be described by a relativistic stopping formula. The stopping power is defined as the energy E lost per unit depth x of penetration. For an ion with charge number q_i travelling at velocity v $(= \beta c)$ through a homogenous material with electron number density n_e, the stopping power is

$$S = -\frac{dE}{dx} = \frac{e^4}{4\pi\epsilon_0^2 m_e c^2}\frac{n_e q_i^2}{\beta^2}\left(\ln\left[\frac{2m_e c^2\beta^2}{I(1-\beta^2)}\right] - \beta^2\right) \tag{12.3a}$$

$$\simeq \frac{e^4}{4\pi\epsilon_0^2 m_e}\frac{n_e q_i^2}{v^2}\ln\left[\frac{2m_e v^2}{I}\right] \quad \text{when} \quad \beta \ll 1, \tag{12.3b}$$

where I is the ionization energy averaged over the energy levels of the target atom, m_e is the electron mass and ϵ_0 is the vacuum permittivity. Note that q_i refers to the ionization state (number of electrons removed) of the incident ion. If the target material has a mass density ρ, atomic number Z, and relative atomic mass A, then $n_e = \rho Z/m_u A$, where m_u is the atomic mass unit. As we might expect, the stopping power increases with the electron number density of the target material and with the charge of the incoming ion. It is also higher for a smaller ionization potential of the target material, as those secondary electrons can then carry energy away. The stopping power does not, however, depend directly on the mass of the incoming ion.

The dependence of the stopping power on velocity for a hydrogen ion incident on three different materials is shown in figure 12.4. For the mean ionization energy I of the target material, I have adopted a common approximation in which I depends only on the atomic

Downloaded from https://www.cambridge.org/core. UNIVERSIDAD AUTONOMA METROPOLITANA, on 13 Nov 2026 at 09:32:29, subject to the Cambridge Core terms of use, available at https://www.cambridge.org/core/terms. https://doi.org/10.1017/9781009700429.013

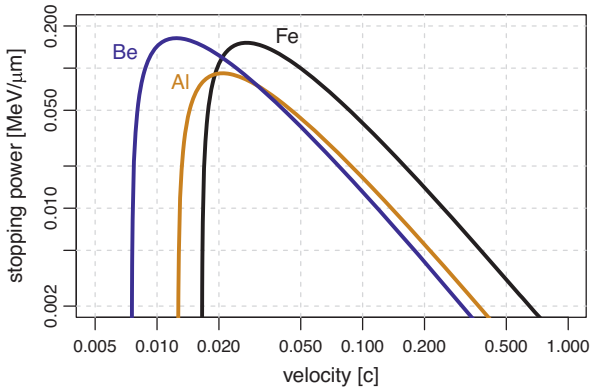


Fig. 12.4 The stopping power as given by equation 12.3a as a function of velocity, for a hydrogen ion ($q_i = 1$) incident on three different materials: iron (Fe, $Z = 26$), aluminium (Al, $Z = 13$) and beryllium (Be, $Z = 4$). For comparison, the energy of a hydrogen ion moving at 0.1 c is 4.7 MeV.

number Z of the target material. Here I use $I = 58\,\text{eV}$ for beryllium, $I = 163\,\text{eV}$ for aluminium, and $I = 541\,\text{eV}$ for iron. In all cases we see that the stopping power is maximum at intermediate velocities, but smaller for low and high velocities.

Equation 12.3a and thus figure 12.4 is an idealized approximation. In real materials we do not see the sharp drop in stopping power at low energies. Furthermore, the target material properties depend on its temperature: at high temperatures, the stopping power is lower and so the penetration depth larger.

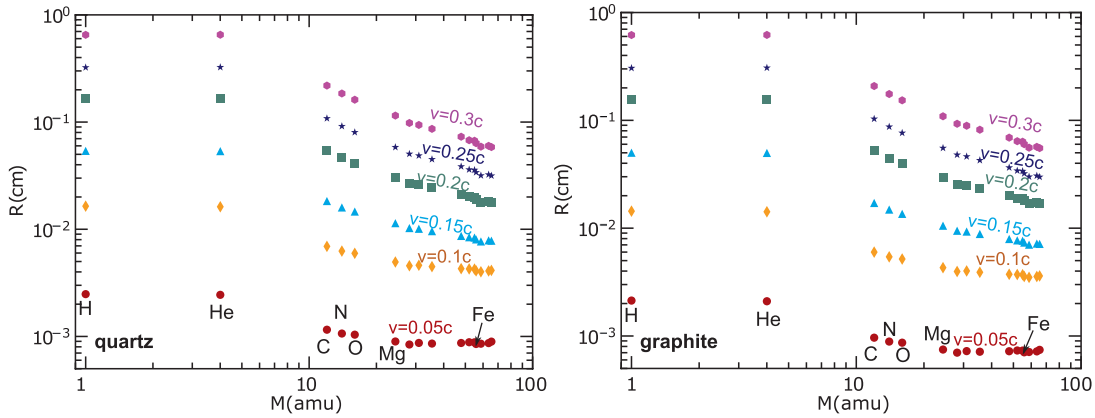
Hoang et al. (2017) used a more sophisticated numerical model to investigate the impact of high-energy ions on materials. They find that light ions like hydrogen and helium ions travelling at 0.1 c transfer about 13 eV to each atom in a target material like quartz or graphite. This is enough to eject a few of the outermost electrons. While these secondary electrons will heat the material, they are insufficient to cause permanent damage. Heavier incident ions like iron ions, in contrast, transfer about 1 keV per atom, so can cause permanent damage along the length of their tracks. The threshold stopping power above which such damage occurs depends on the material, but for silicon it is about $1.5\,\text{MeV}\mu\text{m}^{-1}$ and for graphite about $5.1\,\text{MeV}\mu\text{m}^{-1}$. For very good conductors like copper or diamond, the threshold is very high, possibly infinite. The width of the damage track depends on a number of factors, including the conductivity of the material and the velocity. Good conductors transport heat away more quickly, resulting in a narrower track. Larger velocities generally produce narrower tracks.

By integrating equation 12.3a – or a more accurate expression for the stopping power – we can compute the distance over which an ion is stopped as

$$R = \int_{E_i}^{0} \left(\frac{dE}{dx}\right)^{-1} dE \tag{12.4}$$

where E_i is the kinetic energy of the incident ion. The results of some such more accurate calculations are shown in figure 12.5. At $v = 0.1\,c$, the stopping distance ranges from 0.2 mm for hydrogen ions down to 0.04 mm for heavy ions like iron. The reason heavy ions are stopped in a shorter distance, despite having more energy, is because the stopping power depends on the charge of the incident ion: $S \propto q_i^2$ in equation 12.3a, and we are considering

Downloaded from https://www.cambridge.org/core. UNIVERSIDAD AUTONOMA METROPOLITANA, on 13 Nov 2026 at 09:32:29, subject to the Cambridge Core terms of use, available at https://www.cambridge.org/core/terms. https://doi.org/10.1017/9781009700429.013



Stopping distances of high-energy ions of different masses (horizontal axis) and velocities (colours) incident on quartz (left) and graphite (right). Credit: From Hoang et al. (2017) © AAS. Reproduced with permission. **Fig. 12.5**

complete ionization. At higher velocities, the stopping distance is larger, but is still below 2 mm at $v = 0.2\,c$.

Although impacting electrons do not cause as much direct damage to the spacecraft material as do impacting ions, the electrons are decelerated by interactions with the material, and as a result radiate their kinetic energy as bremsstrahlung. At $v = 0.1\,c$, an electron has a kinetic energy of 2.6 keV, so this is radiated at a range of X-ray wavelengths. These X-rays can damage the spacecraft by ejecting electrons from the atoms. The total X-ray flux from this process is expected to be relatively low, however, and as the electrons will penetrate only to depths of a few nanometres, the X-rays could be shielded without too much difficulty. Decelerating ions also produce bremsstrahlung, but the rate of energy loss by bremsstrahlung scales inversely with the mass, so the X-ray power is much lower. However, ions penetrate more deeply into the material (up to a few millimetres, as we just saw), so its X-rays may be harder to shield.

Although the ISM is overall neutral, a spacecraft can nonetheless acquire a net charge over time. The interactions just described tend to eject more electrons than ions from the spacecraft material, leaving the spacecraft positively charged. Ultraviolet starlight can also lead to the spacecraft becoming positively charged via the photoelectric effect. Spacecraft charging is a problem because it can damage onboard electronics and interfere with scientific measurements. A charged spacecraft would also interact with the ISM's or target star's magnetic field, which could modify the spacecraft's trajectory.

12.4.3 Damage by dust

Figure 12.6 illustrates the impact of a dust particle on a spacecraft. Initially, the particle has enough kinetic energy to unbind the atoms from the surface, that is, to evaporate them. As the particle loses energy through these interactions, it at some point no longer has enough energy to eject any more atoms, but it still has enough energy to break molecular bonds and thus melt the material.

Figure 12.7 shows the result of an experimental impact of a small aluminium sphere with a block of aluminium at an initial relative velocity of 6.8 km s^{-1}. The sphere is much larger

Downloaded from https://www.cambridge.org/core. UNIVERSIDAD AUTONOMA METROPOLITANA, on 13 Nov 2026 at 09:32:29, subject to the Cambridge Core terms of use, available at https://www.cambridge.org/core/terms. https://doi.org/10.1017/9781009700429.013

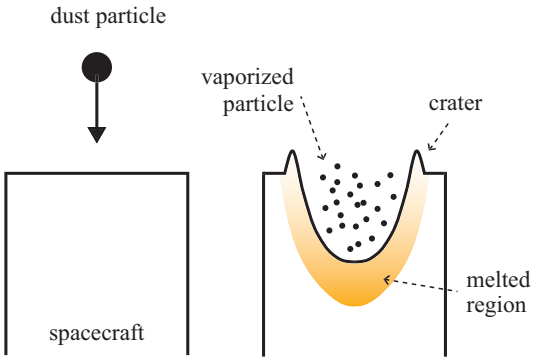


Fig. 12.6 A schematic of a collision of a high-velocity dust particle with a solid. The particle is completely vaporized by the collision and the resulting ions (and electrons, not shown) can continue to penetrate into the solid, heating it and causing subsurface melting.

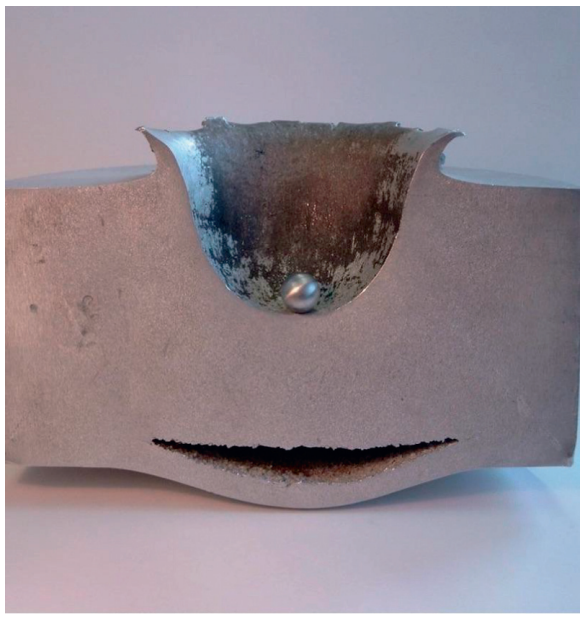


Fig. 12.7 The result of the impact of a 1.2 cm diameter sphere of aluminium (mass 2.4 g) with an aluminium block at a velocity of 6.8 km s^{-1}. The impact vaporizes a significant amount of the block, and also melts some of the surrounding material, which later solidifies. The sphere itself is also vaporized by the impact; the one shown is just for reference. Credit: European Space Agency, ESA Standard Licence.

than a dust particle, and the impact much slower than would occur on a fast interstellar spacecraft. But the photograph illustrates the general principle of what happens.

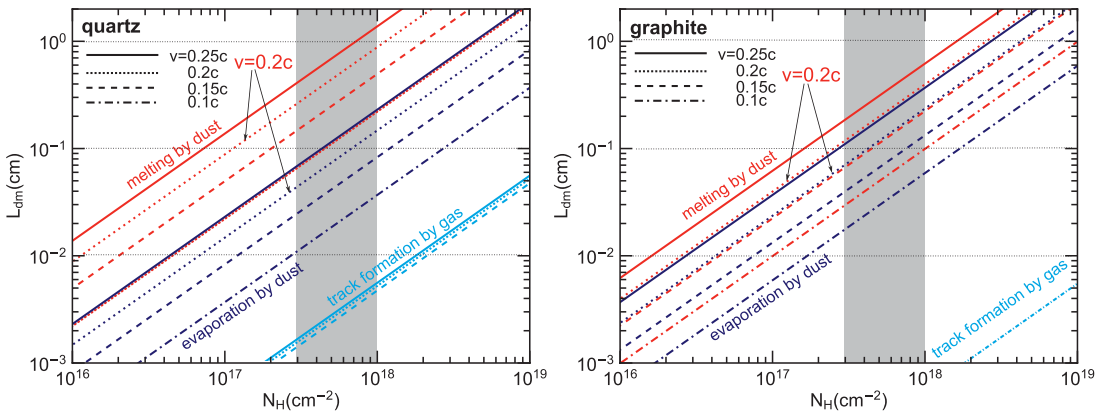
At large velocities, the kinetic energy per atom of the incident dust particle is larger than the binding energy that holds these atoms together as a particle. The impact can therefore be considered as an impact of many atoms simultaneously. As with individual atom impacts discussed in section 12.4.2, each atom is quickly ionized by the impact. The main difference to before is that now a much larger amount of kinetic energy is delivered at the same time.

Downloaded from https://www.cambridge.org/core. UNIVERSIDAD AUTONOMA METROPOLITANA, on 13 Nov 2026 at 09:32:29, subject to the Cambridge Core terms of use, available at https://www.cambridge.org/core/terms. https://doi.org/10.1017/9781009700429.013

We saw in section 12.4.1 that the total ISM dust mass impacting a spacecraft on a journey to Proxima Cen is about 2×10^{-7} kg m^{-2}, so at a relative velocity of 0.1 c this dust would deliver 0.1 GJ m^{-2} of kinetic energy. How much of this energy goes in ionizing, vaporizing, melting, or just heating the target material is a complex process that requires numerical simulation. The amount of material melted, for example, depends on both its thermal conductivity and its melting temperature. The higher the conductivity, the more quickly heat can be dissipated into the rest of the structure, and so the lower the temperature around the point of impact. If the material is melted, this can lead to permanent changes in the material, which would obviously destroy critical structures like electronics, but could also compromise other components. All other things being equal, conductors therefore generally make better shields than insulators, as will materials with higher melting temperatures, provided they can radiate the heat efficiently from the spacecraft. There is some trade-off here, however, because materials with low atomic numbers tend to have higher melting temperatures, whereas materials with higher atomic numbers tend to provide shorter stopping distances and have better heat dissipation.

Figure 12.8 shows the result of one calculation to determine how deeply the surface of a spacecraft is damaged by melting or evaporation by dust impacts. This is shown as a function of the total number of gas particles encountered per unit area over the journey (the fluence). We notice a number of things. First, the depth of damage caused by melting is larger than that caused by evaporation. Second, more damage is done at larger velocities, because the particles have more energy. Third, the damage tracks caused by gas ions are shallower than those of the dust, despite the higher total mass of gas. Finally, graphite, on the right, is less damaged than quartz because it is a better conductor. In either case, this figure shows that a shield of depth of order 1 cm would be enough to prevent damage to components below it during a mission to our nearest star.

Figure 12.8 does not show what fraction of the surface area is eroded or melted by the impacts to this depth. For the typical dust fluence we have been assuming for a journey to



The total depth removed from the surface (L_{dm}) of a quartz (left) or graphite (right) shield as a function of the total number of gas particles encountered per unit area (N_H), assuming a gas-to-dust mass ratio of 100. The red lines indicate melting by dust, the blue lines evaporation by dust, and the orange lines damage by gas, for various velocities (indicated by the line types). The grey region shows the range of the total gas number considered by the authors of the study to be likely encountered on a journey to Alpha Cen. Credit: From Hoang et al. (2017), © AAS. Reproduced with permission.

Fig. 12.8

Downloaded from https://www.cambridge.org/core. UNIVERSIDAD AUTONOMA METROPOLITANA, on 13 Nov 2026 at 09:32:29, subject to the Cambridge Core terms of use, available at https://www.cambridge.org/core/terms. https://doi.org/10.1017/9781009700429.013

Proxima Cen, it turns out that 10% to 100% of the surface area would be vaporized, and 100% of it melted. So the entire area of the shield would be damaged to the depths reported. This implies that we may not want to deploy large unprotected structures, like antenna or telescope mirrors, until close to the destination.

Most of the damage done by dust would probably be done by the largest dust particles, even though these are rarer than small ones. A study by London and Early (2018), for example, showed that a single 10 μm dust particle moving at $v = 0.2\,c$ would require about 1 cm of silicon to stop it, and this would melt 1.6 g of the silicon in the process. Such an impact would be enough to destroy a very small spacecraft of the size considered for an ultralight laser sailcraft (see chapter 11). A 0.3 μm particle would only penetrate to 1.2 mm at $v = 0.2\,c$, but this is reduced to 0.25 mm at $v = 0.1\,c$. The amount of material melted is proportional to the kinetic energy of the dust particle, so a slower spacecraft ($E_k \sim v^2$) and thus longer mission time greatly reduces the damage done.

As the dust particles deliver a lot of kinetic energy to the spacecraft, they will raise the equilibrium temperature of the surface layer. The study of Hoang et al. (2017) shows that at a dust number density of 10^{-7} m^{-3} and velocity of $0.1\,c$, the temperature should remain under 100 K. Even at 10 times this density and twice the velocity, the temperature remains under 300 K.

We saw in the previous section that individual ions will be stopped over a distance of 0.04 mm (for heavy ions) or more (for hydrogen ions). Thus a high-velocity ion or dust particle will pass straight through a very thin layer such as a sail (or perhaps a mirror). In such cases, not all of the energy from the particles will be deposited into the material, so the above calculations of melting and vaporization do not directly apply. But a dust particle would leave a hole in the spacecraft with a size equal to the particle's cross-sectional area. Adopting $d = 0.4$ μm as the typical diameter of a dust particle (section 12.3.2), and $n = 2 \times 10^9$ m^{-2} as the number of dust impacts per unit area over a journey to Proxima Cen (section 12.4.1), then the fraction of the surface area perforated by dust particles is of the order of[5] $n\pi d^2/4 = 3 \times 10^{-4}$. Even if the average dust number density has been underestimated somewhat, a thin sail, for example, should make the journey mostly intact. A small fraction of holes would barely reduce its performance, although the torques of large dust particles might be a problem for navigation and control (see exercises). On the other hand, a sail used only for acceleration early in the mission would not need to be retained once the cruise velocity is attained, and could either be ejected or folded away.

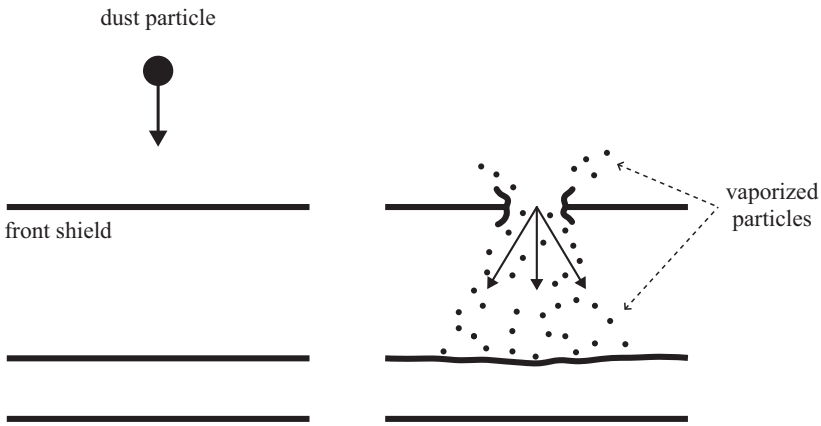
All of the impacting particles – gas and dust – also induce drag on the spacecraft, a topic we examine in section 12.5.

12.4.4 Implications for spacecraft design

As most of the damage from the ISM comes from dust particles in the direction of travel, we should construct a spacecraft with the smallest possible cross-sectional area in that direction. In front of this we can place shielding material with a depth of several millimetres. Ideally this would be a good conductor with a high melting temperature and low density (to keep the mass down), although as noted above, there is a trade-off between high atomic mass solids with larger stopping powers and heat dissipation, and low atomic mass with higher melting

[5] If this number is close to unity, we need a more sophisticated calculation that allows for overlaps.

Downloaded from https://www.cambridge.org/core. UNIVERSIDAD AUTONOMA METROPOLITANA, on 13 Nov 2026 at 09:32:29, subject to the Cambridge Core terms of use, available at https://www.cambridge.org/core/terms. https://doi.org/10.1017/9781009700429.013



A Whipple shield. Dust particles are disintegrated by their impact on the front shield. Although the remnants penetrate this and still have significant energy, they are spread over a larger area and are more easily stopped by the next shield layer.

Fig. 12.9

temperatures. Behind this shield we can place critical components, such as electronics. Damage to passive structures like a sail or antenna may be less critical – a few holes would not make much difference – and if these can be made very thin, then dust particles could pass through them without depositing all of their energy.

Some spacecraft that have visited comets, such as ESA's Giotto and NASA's Stardust, as well the International Space Station in Earth orbit, have used Whipple shields to protect themselves against large dust fluxes. Instead of using one thick piece of material, a Whipple shield uses two or more layers of thinner shields, as shown schematically in figure 12.9. The incident particles penetrate the first shield, but in the process are disintegrated into many smaller pieces. These are then decelerated and eventually absorbed by the next layer, a process that can be repeated with multiple layers to stop particularly large or energetic particles. If the first shield is placed sufficiently far from the rest of the spacecraft, the disintegrated remnants may even spread out enough that some may miss the next layer altogether. In this way the total mass required for shielding can be reduced, although at the expense of a larger volume.

Incoming ions and charged dust particles could be deflected by magnetic or electric fields. Given the larger damage caused by dust particles, deflecting the ions only makes sense if the dust particles can also be deflected. Larger dust particles may be charged, so could in principle be deflected, but the apparatus to do so would presumably be more massive than some extra shielding. However, in chapter 13 we will consider the use of electric and magnetic sails for accelerating spacecraft, and these could also be configured to provide some shielding.

One thing we have not yet mentioned is that very high energy particles, in particular cosmic rays, can produce neutrons when they impact the spacecraft by the process of nuclear spallation. These neutrons can then go on to damage the spacecraft structure, and neutron capture by atoms in the spacecraft can result in unstable isotopes that then decay radioactively. This is the problem of neutron activation that we also encountered with nuclear rockets in section 8.5.1.

Downloaded from https://www.cambridge.org/core. UNIVERSIDAD AUTONOMA METROPOLITANA, on 13 Nov 2026 at 09:32:29, subject to the Cambridge Core terms of use, available at https://www.cambridge.org/core/terms. https://doi.org/10.1017/9781009700429.013

12.5 Drag on a spacecraft

The ISM particles that collide with a spacecraft have momentum. This drag will cause the spacecraft to decelerate.

Consider a spacecraft of mass M with cross-sectional area A travelling at a velocity v relative to the ISM of mass density ρ. Over distance dx (measured in the ISM rest frame) the spacecraft collides with mass $dm = \rho A dx$. Assuming these particles are stopped by the spacecraft (rather than pass through it or are elastically reflected), they impart momentum $dp = -\gamma v dm$ (equation 7.8). The force on the spacecraft in the ISM rest frame is therefore $F = dp/dt = -\rho A \gamma v^2$, as $v = dx/dt$. Assuming further that the mass of the spacecraft remains constant (the particles are brought to a halt but do not stick), then from equation 7.25 the proper acceleration of the spacecraft due to the drag is

$$a' = -\frac{\rho A}{M} \gamma v^2 \,. \tag{12.5}$$

Recall that the proper acceleration is what the spacecraft experiences in its instantaneous rest frame. Figure 12.10 shows how the velocity-dependent term in the drag varies with velocity. Adopting round values of $\rho = 10^{-21}\,\mathrm{kg\,m^{-3}}$ (Table 12.1), $A = 1\,\mathrm{m}^2$, $M = 1\,\mathrm{kg}$, and $v = 0.2\,\mathrm{c}$, we find that $a' = -3.7 \times 10^{-6}\,\mathrm{m\,s^{-2}}$. The coordinate acceleration of the spacecraft in the ISM rest frame is obtained via the Lorentz transformation as a'/γ^3 (equation 7.15). On account of the much larger density of gas than dust in the ISM, gas rather dominates the drag (whereas dust dominates the damage).

Integrating the coordinate acceleration we can determine how the velocity changes with distance due to the drag. For $\beta < 0.2$ we have $\gamma \simeq 1$, which makes the calculation easier. Separating the variables we get

$$\int \frac{dv}{v} = -\int \frac{\rho A}{M} dx, \tag{12.6a}$$

$$\frac{v}{v_0} = \exp\left(-\frac{\rho A}{M} x\right), \tag{12.6b}$$

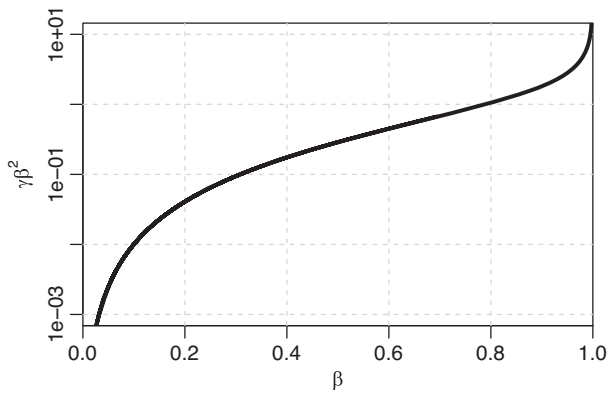


Fig. 12.10 The drag on a spacecraft, its proper acceleration is $-\frac{\rho A}{M} c^2 \gamma \beta^2$.

Downloaded from https://www.cambridge.org/core. UNIVERSIDAD AUTONOMA METROPOLITANA, on 13 Nov 2026 at 09:32:29, subject to the Cambridge Core terms of use, available at https://www.cambridge.org/core/terms. https://doi.org/10.1017/9781009700429.013

where v_0 is the initial velocity and x is the distance travelled. Using the above values and $x = 4.25\,\text{ly}$, the term in the exponential is -4×10^{-5} and so $v/v_0 \simeq 1$. The velocity is hardly changed at all. If we instead had a sailcraft with a lightness number $\lambda = 1$, and thus a loading parameter $\sigma = M/A = 1.53 \times 10^{-3}\,\text{kg}\,\text{m}^{-2}$ (section 10.2), we have $\rho(A/M)x = -0.027$, and thus $v/v_0 = 0.973$, a very modest reduction in the velocity. In conclusion, drag from the ISM will not significantly slow down any moderately fast spacecraft over the distances to the nearest stars. However, even a small increase in travel time, and thus a later arrival time, caused by the drag has a significant impact on navigation, as we will see in chapter 14.

12.6 The Bussard ramjet

The big drawback of a rocket is that it has to carry its fuel. This limits its velocity to a few times its effective exhaust velocity in practice. Solar and laser sails overcome this by using externally provided photons as the source of momentum. Solar-electric ion engines partly overcome this by getting energy from an external source, but they still take their propellant with them. Are there other external sources we could use for both energy and momentum?

The ISM contains gas at a very low mass density, predominantly hydrogen atoms and ions. If we could collect these and force them to undergo fusion, this would release energy that accelerates the fusion products, as in a nuclear rocket. This is the idea of the Bussard ramjet. How the fusion might be achieved will be discussed later. Let us first look at the overall principle.[6]

12.6.1 Principle

Figure 12.11 sketches the idea of a Bussard ramjet. When a spacecraft moves at velocity β relative to the ISM, it sweeps up matter using a large collector of cross-sectional area A. With matter density ρ, then over distance dx the mass collected is $dm = \rho A dx$. Note that dx is measured in the ISM rest frame. In terms of the time dt in the ISM rest frame we have $dx = c\beta dt$. In order to make some of the expressions below more compact, in this section I use the (dimensionless) proper velocity $\omega = \gamma\beta$ (see equation 7.20). As we shall derive an expression for the proper acceleration, it will be convenient to express dm in terms of the proper time interval dt' on board the spacecraft. The relation between the two times is the time dilation, $dt = \gamma dt'$ (equation 7.11). The mass swept up by the ramjet in time dt' is therefore

$$dm = \rho A c \omega dt' \,. \tag{12.7}$$

Suppose the ramjet brings dm to rest relative to the spacecraft and converts a fraction ϵ of this mass into energy, which is used to propel the spacecraft. In general this propellant would be a combination of matter particles and photons, and so we have a situation rather similar to the mixed matter–photon rocket discussed in section 7.8, although we will start here from

[6] A conventional ramjet is a type of air-breathing jet engine that uses the high velocity of the aircraft to compress air, which is then heated by fuel combustion to produce the propelling jet. This contrasts with turbojet and turbofan engines on most modern aircraft that use a gas turbine to compress the air. A ramjet only works once the aircraft is flying fast enough that an additional compression is not required, typically at supersonic speeds.

Downloaded from https://www.cambridge.org/core. UNIVERSIDAD AUTONOMA METROPOLITANA, on 13 Nov 2026 at 09:32:29, subject to the Cambridge Core terms of use, available at https://www.cambridge.org/core/terms. https://doi.org/10.1017/9781009700429.013

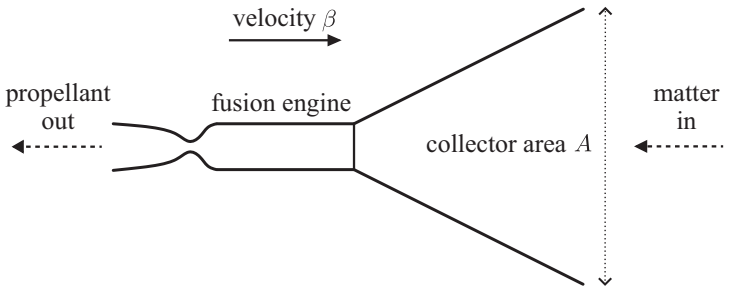


Fig. 12.11 A Bussard ramjet moving at velocity β relative to the ISM. The collector of cross-sectional area A collects mass. This is made to undergo nuclear fusion, and the high-velocity propellant is ejected out of the back.

first principles. We assume the mass of the spacecraft remains constant at M, and that there are no energy losses ($\eta = 1$ in the context of section 7.8).

In the ISM rest frame, the increase in the (kinetic) energy of the spacecraft is the energy provided by matter conversion minus the energy E_j that goes into the propellant jet:

$$dE = \epsilon c^2 dm - E_j \, . \tag{12.8}$$

The change in the momentum of the spacecraft dp is the momentum gained by ejecting the propellant, which is equal in magnitude and opposite in direction to the momentum of the propellant p_j, minus the momentum of the absorbed ISM matter, which is $\gamma v dm$. This latter term is the drag we discussed in section 12.5. Using the proper velocity we get

$$dp = p_j - \omega c dm \, . \tag{12.9}$$

Assuming dp is initially positive, equation 12.9 tells us that the spacecraft will accelerate, ω increases, and so the spacecraft will collect more matter per unit time (equation 12.7). Will it continue to accelerate indefinitely? Yes, but by ever decreasing amounts, because assuming p_j is constant (i.e. we extract the same momentum per unit mass), then as ω increases, dp decreases, eventually to zero. The spacecraft approaches a maximum velocity asymptotically due to the drag.

To proceed we consider the two limiting cases, first a photon-only propellant jet, and then a matter-only propellant jet.

Stopping matter: photon jet

Here the mass ϵdm is used to produce photons of energy E_j (relative to the rocket) that are collimated into a jet out of the back of the spacecraft, as with the photon rocket. The remaining mass, $(1 - \epsilon)dm$, is dumped overboard at zero velocity relative to the spacecraft. To find the asymptotic proper velocity ω_∞, we set $dE = 0$ and $dp = 0$ in equations 12.8 and 12.9. As $E_j = cp_j$ for photons, we get

$$\omega_\infty = \epsilon \quad \text{(photon jet)}. \tag{12.10}$$

The asymptotic proper velocity equals the fraction of the collected mass converted into photon energy. One of the highest values of ϵ for a fusion reaction is the proton–proton (p–p)

Downloaded from https://www.cambridge.org/core. UNIVERSIDAD AUTONOMA METROPOLITANA, on 13 Nov 2026 at 09:32:29, subject to the Cambridge Core terms of use, available at https://www.cambridge.org/core/terms. https://doi.org/10.1017/9781009700429.013

chain, which converts hydrogen to helium (equation 8.4) and has $\epsilon = 0.007$. Although this reaction does not put much of the energy released into the photons, if this energy could nonetheless be converted into a photon jet, the ramjet would reach an asymptotic velocity of $\beta = 0.007$. To achieve a higher ϵ, we would have to use antimatter (section 8.8.1), but this hardly exists in the ISM.

Stopping matter: mass jet

Let us instead assume that the converted mass–energy $\epsilon c^2 dm$ is used to accelerate the remaining mass $(1-\epsilon)dm$ as propellant (instead of dumping it overboard). No photons are produced. The energy and momentum of a mass jet are

$$E_j = (1-\epsilon)(\gamma_j - 1)c^2 dm \quad \text{and} \tag{12.11a}$$

$$p_j = (1-\epsilon)c\omega_j dm, \tag{12.11b}$$

where γ_j and ω_j refer to the velocity of the jet relative to the ISM. Proceeding as before, we find that the asymptotic velocity is

$$\omega_\infty = \sqrt{\epsilon(2-\epsilon)} \quad \text{(mass jet)}. \tag{12.12}$$

With $\epsilon = 0.007$, the asymptotic velocity is $\beta = 0.117$, considerably higher than for the photon jet. The variation of the asymptotic velocity with ϵ is shown in figure 12.12. For both the photon jet and the mass jet, the maximum asymptotic proper velocity, achieved when $\epsilon = 1$, is $\omega_\infty = 1$, which corresponds to $\beta = 1/\sqrt{2} = 0.71$. This could not be achieved using known matter available in the ISM, however.

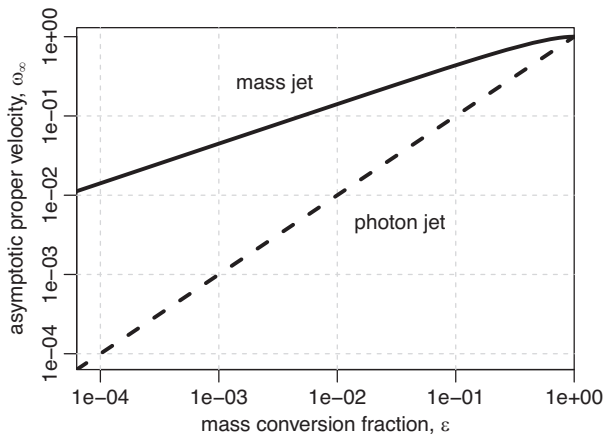


Fig. 12.12 The asymptotic proper velocity of a Bussard ramjet when stopping the incoming matter in the spacecraft as a function of the fraction of mass converted to energy, for a photon jet (dashed line, equation 12.10) and a mass jet (solid line, equation 12.12).

Downloaded from https://www.cambridge.org/core. UNIVERSIDAD AUTONOMA METROPOLITANA, on 13 Nov 2026 at 09:32:29, subject to the Cambridge Core terms of use, available at https://www.cambridge.org/core/terms. https://doi.org/10.1017/9781009700429.013

Acceleration

So far we have assumed that the matter must be stopped in the spacecraft for fusion to occur. If this could somehow be avoided (see below), then we can drop the drag term from equation 12.9. As the mass of the spacecraft is constant, the expressions for the change of energy and momentum in the ISM rest frame (equations 12.8 and 12.9) can now be written

$$dE = d\gamma Mc^2 = \epsilon c^2 dm - E_j \quad \text{and} \tag{12.13a}$$

$$dp = d\omega Mc = p_j. \tag{12.13b}$$

As there is no drag, it's clear from the second equation above that the proper velocity is no longer limited, and so the spacecraft will asymptotically approach the speed of light. We can find how quickly this happens by computing the proper acceleration. From equation 7.26 this is

$$a' = \frac{c}{\gamma}\frac{d\omega}{dt'}\,. \tag{12.14}$$

Let us compute this for the photon jet and mass jet cases. In doing this we use the relation $\gamma^2 = 1 + \omega^2$, from which we also get $\gamma d\gamma = \omega d\omega$.

Not stopping matter: photon jet

For photons, $E_j = p_j c$. Using this to combine equations 12.13b we get

$$M\left(\frac{\omega}{\gamma} + 1\right) d\omega = \epsilon\, dm\,. \tag{12.15}$$

Using equation 12.7 for dm, the proper acceleration is

$$a'_{\text{no drag}} = \frac{\rho A c^2}{M}\frac{\epsilon\omega}{(\omega+\gamma)} = \frac{\rho A c^2}{M}\frac{\epsilon\beta}{(1+\beta)} \quad \text{(photon jet)}. \tag{12.16}$$

Figure 12.13 illustrates how this acceleration varies with the velocity for the cases $\epsilon = 0.007$ and $\epsilon = 1$. In this log–log plot, we see a near-linear increase up to an asymptotic non-zero acceleration of $\epsilon\rho A c^2/2M$. Thus, as long as the spacecraft sweeps up and fuses matter, its asymptotic velocity is the speed of light.

Had we retained the drag term ($-\omega c dm$) in this derivation, we would get $\epsilon - \omega$ in place of ϵ in equation 12.16. This acts to decelerate the spacecraft when $\omega > \epsilon$, and gives zero acceleration when $\omega = \epsilon$, which is just the asymptotic velocity we found before (equation 12.10).

Not stopping matter: mass jet

For a mass jet, we use equations 12.11b for E_j and p_j in equations 12.13b. The maths is slightly more complicated, and results in a quadratic equation for the acceleration. The solution is

$$a'_{\text{no drag}} = \frac{\rho A c^2}{M}\,\omega\left[\sqrt{\omega^2 + \epsilon(2-\epsilon)} - \omega\right] \quad \text{(mass jet)}. \tag{12.17}$$

This is plotted as a function of velocity for $\epsilon = 0.007$ as the solid line in figure 12.13. The behaviour is qualitatively similar to the photon jet, but the mass jet reaches a higher asymptotic acceleration than the photon jet, and reaches this already at a lower velocity.

Downloaded from https://www.cambridge.org/core. UNIVERSIDAD AUTONOMA METROPOLITANA, on 13 Nov 2026 at 09:32:29, subject to the Cambridge Core terms of use, available at https://www.cambridge.org/core/terms. https://doi.org/10.1017/9781009700429.013

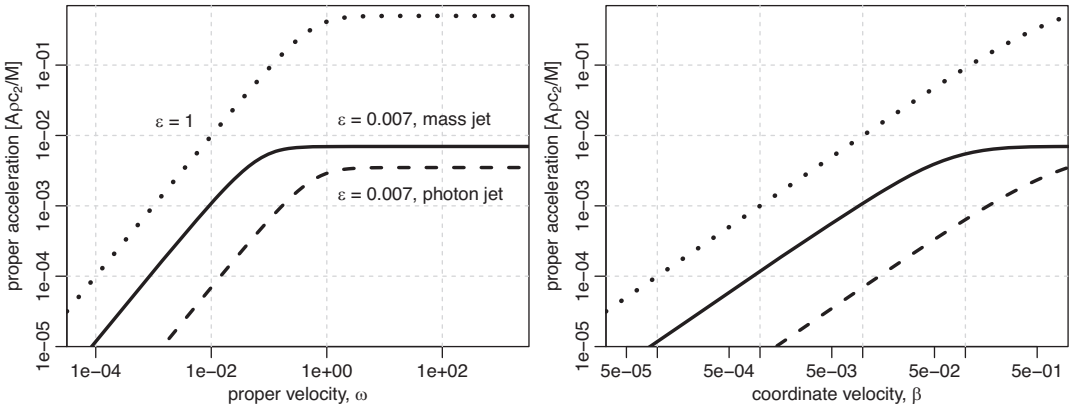


Fig. 12.13 The variation of the proper acceleration of the Bussard ramjet with proper velocity (left) and coordinate velocity (right) when the incoming matter it not stopped. The dashed and solid lines are for a photon ramjet (equation 12.16) and a mass-ejecting ramjet (equation 12.17), respectively, both for $\epsilon = 0.007$. The dotted line is for 100% conversion of mass to energy ($\epsilon = 1$) for the photon ramjet, which is also the limit of the mass-ejecting ramjet.

When $\epsilon = 1$, equations 12.16 and 12.17 are identical, although the mass-ejecting ramjet is then converting all of the matter into energy, leaving nothing to eject, so this is only a theoretical limiting case.

12.6.2 A ramjet's journey

From the expressions for the acceleration in terms of the proper velocity derived above, we can integrate equation 12.14 to determine the proper time taken to accelerate from from ω_i to ω_f:

$$t'_f = c \int_{\omega_i}^{\omega_f} \frac{d\omega}{\gamma a'} \,. \tag{12.18}$$

This has a closed-form solution, but it's rather complex, so here I just integrate numerically for a range of ω_f values to get a corresponding set of t'_f values. This gives us the variation of velocity with time as the spacecraft accelerates.

Using the definition of proper velocity we can integrate again to get the distance travelled in a given time

$$x_f = c \int_0^{t'_f} \omega dt' \,. \tag{12.19}$$

We can compute this by numerical integration too. Given a sufficiently dense list of (t'_f, ω_f) values from the first integral, we can compute x_f for each of these using the trapezium rule or Simpson's rule.

Let us compute the flight profile for a drag-free Bussard ramjet, for both the photon jet and mass jet scenarios. We assume the ramjet sweeps up and fuses hydrogen via the p–p chain, so $\epsilon = 0.007$. The spacecraft travels through the local interstellar cloud (table 12.1), which we take to have a gas number density of $0.3 \times 10^6\,\mathrm{m}^{-3}$. Most of this is hydrogen, so we adopt a density of fusionable matter of $\rho = 5 \times 10^{-22}\,\mathrm{kg\,m}^{-3}$ (and ignore the drag of the non-fusionable material).

Downloaded from https://www.cambridge.org/core. UNIVERSIDAD AUTONOMA METROPOLITANA, on 13 Nov 2026 at 09:32:29, subject to the Cambridge Core terms of use, available at https://www.cambridge.org/core/terms. https://doi.org/10.1017/9781009700429.013

The mass of the spacecraft comprises the mass of the collector and the mass M_p of everything else ('payload', for brevity). The collector has constant cross-sectional areal mass density σ, and so its mass is σA. The acceleration scales as $\rho A/M$, so if the collector dominated the spacecraft's mass budget, the acceleration would scale as ρ/σ. In general we have $M = \sigma A + M_p$, so the acceleration scales instead as $\rho/(\sigma + M_p/A)$. As M_p must include a fusion engine, it is probably not going to be small. No such engine exists, so I will make a wild (and probably very optimistic) guess and assume this has a mass of 10^3 kg. The collector would presumably be some kind of wire mesh that electromagnetically captures hydrogen ions. I will somewhat arbitrarily assume $\sigma = 1.53 \times 10^{-4}\,\mathrm{kg\,m^{-3}}$, which if it were a solar sail corresponds to a lightness number of 10 (equation 10.10). Adopting a circular collector of radius 3 km, we have $M_p/A = 3.5 \times 10^{-5}\,\mathrm{kg\,m^{-3}}$, which is four times less than σ, and so the payload is not the limiting factor. A much larger collector therefore brings little benefit, because the extra collecting area would serve mostly to accelerate the extra mass of this collecting area. A larger collector presumably also means we need a larger engine to process the higher flux of protons, and thus a higher mass payload.

With these assumptions, we have $\rho A/M = 2.6 \times 10^{-18}\,\mathrm{m^{-1}}$. The acceleration scales with this quantity, so we can trade off the individual quantities to achieve the same acceleration. For example, if the ISM density is higher by some factor, we could increase the spacecraft mass or lower the collector area by the same factor.

A ramjet only works once it is moving relative to the ISM. We assume our spacecraft starts in Earth's orbit about the Sun with an initial velocity of $30\,\mathrm{km\,s^{-1}}$ relative to the ISM.[7] We now have enough information to compute the above integrations. The resulting variation of the acceleration, velocity, and distance with the proper time for both the mass jet and the photon jet variations are shown in figure 12.14, as well as a constant acceleration case for comparison. The photon jet shows far inferior performance to the mass jet, so we will only discuss the results for the mass jet.

To get to Proxima Cen, our ramjet requires 1650 years of proper time (spacecraft time). At this point, the spacecraft is moving with proper velocity $\omega = 0.012$, which corresponds to coordinate velocity $0.012\,c$ or $3610\,\mathrm{km\,s^{-1}}$. These are almost equal because the spacecraft is barely relativistic.

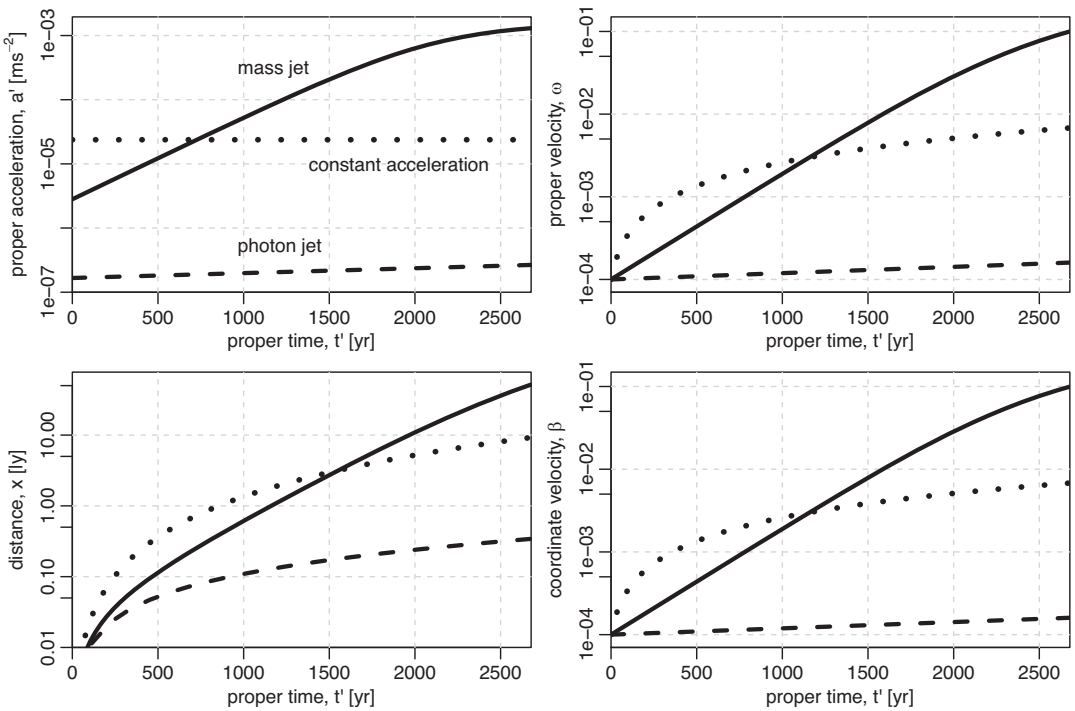
With the same spacecraft, increasing the initial velocity increases the rate of matter consumption and therefore the acceleration. Suppose we used the Oberth effect in a close dive to the Sun (section 4.2.3) to increase the initial velocity to $200\,\mathrm{km\,s^{-1}}$. In that case the time to Proxima Cen decreases to 1025 years, but the velocity at encounter is very similar ($3760\,\mathrm{km\,s^{-1}}$).

To increase the acceleration for given ϵ and ρ, we have to reduce the collector areal density σ. Reducing the payload mass M_p or increasing the area A of the collector do not help much in the adopted scenario, because the collector already dominates the mass. If we could reduce σ so far that $\rho A/M$ increases by a factor of 50, we find that the time taken to Proxima Cen decreases to 72 years. The spacecraft is moving at $0.24\,c$ as it passes the star.

In the original scenario, our spacecraft takes a long time to reach Proxima Cen and is not travelling particularly fast when it does. But it will keep on going, and because the acceleration never decreases to zero, it can eventually reach very high speeds. We see this in

[7] The Sun has a non-zero velocity relative the mean of the ISM, so the initial velocity would vary according to the initial direction the spacecraft travels.

Downloaded from https://www.cambridge.org/core. UNIVERSIDAD AUTONOMA METROPOLITANA, on 13 Nov 2026 at 09:32:29, subject to the Cambridge Core terms of use, available at https://www.cambridge.org/core/terms. https://doi.org/10.1017/9781009700429.013



The variation of the acceleration, proper and coordinate velocities, and distance travelled as a function of proper time for a Bussard ramjet using either a photon jet (equation 12.16, dashed line) or a mass jet (equation 12.17, solid line) when the swept-up matter is not stopped (no drag). The proper and coordinate velocities are almost identical because the spacecraft barely reaches relativistic velocities. This simulation adopts $\rho A c^2/M = 0.24\,\mathrm{m\,s^{-2}}$ (the numerical term in the acceleration equations) and $\omega_i = 10^{-4}$. For comparison, the dotted line shows the case of a constant proper acceleration of $2.4 \times 10^{-5}\,\mathrm{m\,s^{-2}}$.

Fig. 12.14

figure 12.15, where the integration is now extended to much longer times. The acceleration of the mass jet gets close to its asymptotic value after about 3000 years, when it is travelling at nearly half the speed of light (coordinate velocity) and is 100 ly from the Earth. Now that the velocities are relativistic, we see a big difference between the proper velocity and the coordinate velocity (note also the different axis scales in figure 12.15). After 36 000 years of spacecraft time, the spacecraft has covered one million light years and is moving at nearly the speed of light: $\beta = 0.999985$ or $\omega = 180$. This is the regime where the proper velocity is a more convenient measure than the coordinate velocity.

The problem with the Bussard ramjet is how to stop, or at least to decelerate. In principle this could be done by turning the mass (or photon) jet into the direction of travel. Recall that in the above scenario we assumed the matter is not stopped before undergoing fusion, that is, there is no drag from the ISM, so by additionally stopping the matter we could achieve a larger deceleration. The spacecraft could also also be steered through regions of higher ISM density, such as star-forming regions, to achieve a larger deceleration (or acceleration).[8]

[8] The Bussard ramjet is the centrepiece of the novel *Tau Zero* by Poul Anderson. The spacecraft carries a large human crew and is designed to reach an asymptotic acceleration of $1g$. Things get even more interesting after something breaks, and the crew have no way of stopping the acceleration …

Downloaded from https://www.cambridge.org/core. UNIVERSIDAD AUTONOMA METROPOLITANA, on 13 Nov 2026 at 09:32:29, subject to the Cambridge Core terms of use, available at https://www.cambridge.org/core/terms. https://doi.org/10.1017/9781009700429.013

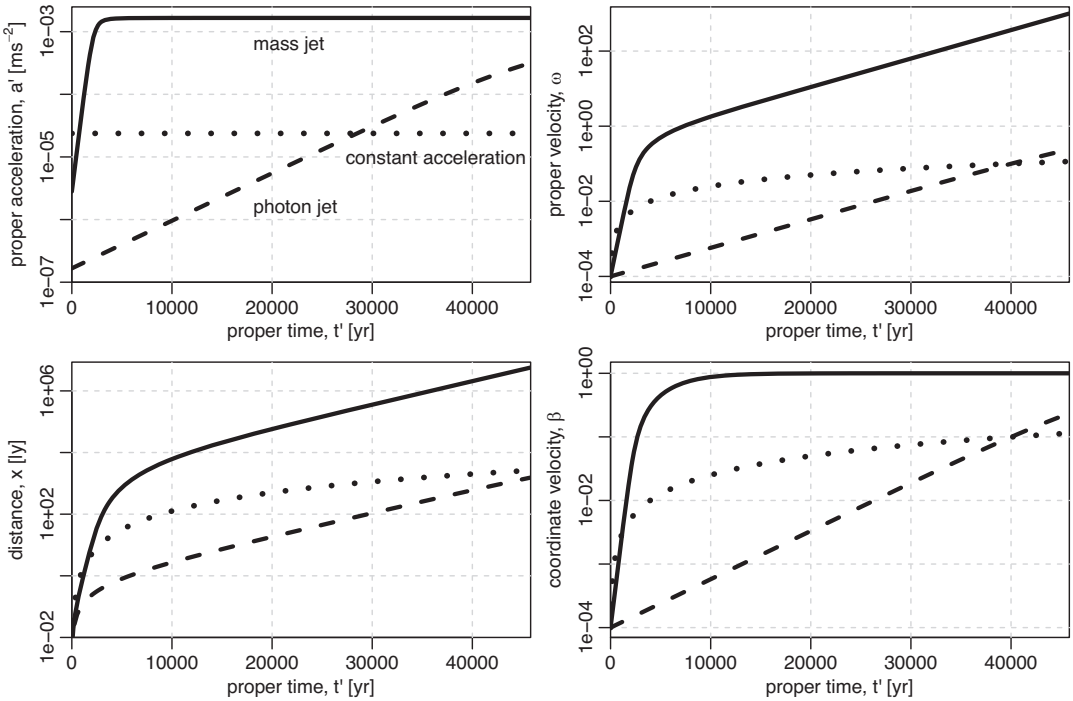


Fig. 12.15 As Fig 12.14 but extended to longer times.

12.6.3 Challenges

We have skipped some important details of ramjets, not least how we actually achieve fusion, especially when not stopping the protons. The value of $\epsilon = 0.007$ adopted implies use of the p–p chain outlined in section 8.5. This is an extremely slow reaction, whereas we have been implicitly assuming fusion would occur as fast as required. An alternative is to use the carbon–nitrogen–oxygen (CNO) cycle. This is the process that converts hydrogen to helium in higher-mass stars. It is much faster than the p–p chain, but it requires a higher temperature of around 15 million kelvins as opposed to about 4 million kelvins for the p–p chain. Furthermore, it requires carbon to get the cycle going, although as the carbon itself is not used up, it is a catalyst in this reaction. Thus the carbon could be taken along by the spacecraft rather than collected from the ISM.

An alternative to hydrogen burning it to use deuterium (^{2}H) fusion, for example in the D+D reaction we considered for a fusion rocket (equation 8.8). Relatively speaking, this is easier to achieve than the CNO cycle. But the deuterium abundance in the ISM is around a factor of 10^5 lower than the hydrogen (^{1}H) abundance, which lowers ρ by this factor.

Another significant challenge is how to collect the interstellar material. If this is done with a magnetic field, then this will only collect the ionized particles in the ISM (around 25% by number near to the Sun). One study, under the name of the Fishback ramjet, examined in detail how this collection could work. It found not only that the collector would have to be enormous (thousands of kilometres) but also that the asymptotic velocity of the ramjet (with drag) would be significantly lower than the simpler, idealized calculations shown above.

Downloaded from https://www.cambridge.org/core. UNIVERSIDAD AUTONOMA METROPOLITANA, on 13 Nov 2026 at 09:32:29, subject to the Cambridge Core terms of use, available at https://www.cambridge.org/core/terms. https://doi.org/10.1017/9781009700429.013

One way to overcome the low-density fuel problem is to send a precursor mission to drop much higher-density fuel pellets along the intended path of the Bussard ramjet, like a trail of breadcrumbs. The obvious problem with this, however, is that we need an additional mission to achieve it. If the path length over which the fuel must be dropped is large, then we already need a fast interstellar mission (not using a ramjet) to achieve another fast interstellar mission (with a ramjet). It would further require that the positions and velocities of the pellets are all carefully coordinated so that they are in the right place at the right time for the intended ramjet trajectory.

The results presented in the previous section assumed that the ISM matter does not have to be stopped to be fused. Current approaches to fusion require high plasma temperatures, densities, and/or confinement times (the Lawson criterion), and it's unclear how we could force fusion in matter travelling at a large velocity relative to the spacecraft. One idea is to use an electric field to decelerate the ionized incoming matter to rest with respect to the spacecraft, and to store this kinetic energy as electric energy in a capacitor. This energy is then given back to the fusion products to accelerate them to higher exhaust velocities than achieved just by the released fusion energy. This effectively removes the ion drag by returning the momentum absorbed to the exhausted propellant.

12.7 Summary

The ISM is made up of neutral atoms, ions, electrons, molecules, dust particles, and macroscopic-sized interstellar objects. Their space densities vary by orders of magnitudes across the Galaxy, but close to the Sun the gas number density is of order $0.3 \times 10^6\,\mathrm{m}^{-3}$. This is mostly hydrogen (90% by number) and helium (9.9%), which corresponds to an overall mass density of $6 \times 10^{-22}\,\mathrm{kg\,m}^{-3}$. About 25% of the hydrogen is ionized. Dust makes up about a hundredth of the mass of the gas, with particle sizes spanning orders of magnitudes.

An interstellar spacecraft will encounter ISM particles at very high velocities. These can cause serious damage by melting or evaporating the surface and through the creation of secondary energetic particles. Although massive atoms like iron are far less abundant than light ones like hydrogen or helium, the massive ones do comparatively more damage. Dust particles are the most serious problem overall on account of their much larger masses, despite being even rarer.

Fortunately, it appears that several millimetres of shielding material, which will be eroded during the journey, is enough to protect a spacecraft against the most likely dust particles encountered. Above some size, a dust particle will be too large to shield and could destroy the spacecraft. As the particle size distribution is poorly known, it is difficult to estimate how likely this is, but it appears unlikely. To reduce the risk, the spacecraft should have the smallest cross-sectional area possible in the direction of travel. Large, thin structures like sails will inevitably be perforated by larger dust particles, but only a small fraction of the surface would be affected on a journey to Proxima Cen.

The solar system is surrounded by a weakly bound, roughly spherical distribution of icy minor bodies with sizes between metres and kilometres. This Oort cloud may extend to a light year from the Sun. Similar structures presumably surround other stars. The space density of the Oort cloud is far too low for it present a hazard to a spacecraft, however.

Downloaded from https://www.cambridge.org/core. UNIVERSIDAD AUTONOMA METROPOLITANA, on 13 Nov 2026 at 09:32:29, subject to the Cambridge Core terms of use, available at https://www.cambridge.org/core/terms. https://doi.org/10.1017/9781009700429.013

Finally, the hydrogen in the ISM could in principle be swept up by a spacecraft and used in a fusion engine as a source of energy and propellant. This so-called Bussard ramjet requires a collector many kilometres in size (perhaps thousands) to collect enough matter to produce adequate acceleration for a sub-century journey to Proxima Cen. How the spacecraft would collect the matter and then fuse it efficiently remains undetermined, so this remains a very far-fetched idea.

12.8 Exercises

1. Using equation 12.1 and the data on the Oort cloud in section 12.1, estimate the probability that an interstellar spacecraft will collide with an Oort cloud comet on its journey outwards. For simplicity, assume that the comets are stationary. Is that valid? How, qualitatively, would the estimate change if this assumption were not valid? If a spacecraft has to pass within one million kilometres of an Oort cloud object to observe it, what is the probability that it would observe at least one during its journey?
2. Figure 12.4 shows that the stopping power of a spacecraft's shield to incident ions has a maximum at intermediate velocities. To get to 0.1–0.2 c, a spacecraft must first accelerate through lower velocities where the stopping power is lower. Might it be that ions cause more damage in this phase than when the spacecraft is moving faster?
3. In section 12.5 we found that the coordinate deceleration due to particle drag on a moving spacecraft is proportional to β^2/γ^2. Plot this against β. Is anything unexpected? From this, derive how the spacecraft velocity varies with distance travelled x, that is, find the relativistic version of equation 12.6b.
4. A flat circular laser sail 2 m in diameter of mass 0.01 kg is hit on its edge by a proton travelling normally to the surface at speed 0.1 c. This exerts a torque that makes the sail rotate. What angular velocity does the sail acquire, assuming the proton sticks to the sail? Is this a problem for navigation and control? What about when it is hit by a dust particle of mass 10^{-16} kg instead?
5. Derive the expressions for the asymptotic velocity of the Bussard ramjet in the photon jet case (equation 12.10) and mass jet case (equation 12.12).
6. Derive equation 12.17.
7. Extend the derivation of the distance travelled and time required to reach a given velocity in section 12.6.2 to the case of having to stop the incoming ISM matter. You first need to write down the expression for the acceleration of the ramjet when including the drag term, and then perform the numerical integrations.

Downloaded from https://www.cambridge.org/core. UNIVERSIDAD AUTONOMA METROPOLITANA, on 13 Nov 2026 at 09:32:29, subject to the Cambridge Core terms of use, available at https://www.cambridge.org/core/terms. https://doi.org/10.1017/9781009700429.013